Establishing a Celestial VLBI Reference Frame—I. Searching for VLBI Sources

R. A. Preston, D. D. Morabito, J. G. Williams, M. A. Slade, A. W. Harris,
S. G. Finley, L. J. Skjerve, and L. Tanida
Tracking Systems and Applications Section

D. J. Spitzmesser
Deep Space Network Operations Section

B. Johnson
Aeronutronics Ford, Newport Beach, California

D. L. Jauncey
C.S.I.R.O., Division of Radiophysics, Sydney, NSW, Australia

A. Bailey, R. Denise, J. Dickenson, R. Livermore,
A. Papij, A. Robinson, and C. Taylor
Tidbinbilla Deep Space Communications Complex, Australia

F. Alcazar, B. Luaces, and D. Munoz
Madrid Deep Space Communications Complex, Spain

The Deep Space Network is currently engaged in establishing a new high-accuracy VLBI celestial reference frame. This article discusses the present status of the task of finding suitable celestial radio sources for constructing this reference frame. To date, 564 VLBI sources have been detected, with 166 of these lying within 10° of the ecliptic plane. The variation of the sky distribution of these sources with source strength is examined.

I. Introduction

The Deep Space Network (DSN) is currently engaged in establishing a new high-accuracy celestial reference frame composed of compact extragalactic radio sources, principally quasars. These radio sources are observed by means of the technique of Very Long Baseline Interferometry (VLBI), whereby two antennas separated by distances of up to an earth diameter, simultaneously observe the same source (Ref. 1). This article will discuss the effort which has been undertaken to find a suitable set of celestial radio sources from which the VLBI reference frame may be constructed.

In the past, astrometric or geodetic studies which required the use of a celestial reference frame had to rely on an optical star reference frame (that is, a set of optical stars whose relative positions were well known). Such reference frames were limited to accuracies of about 0.1 arcseconds (5×10^{-7} radians) in relative source positions due to the effects of atmospheric turbulence on optical observations and the relative angular ("proper") motions of the stars in the sky. Since VLBI sources are extragalactic and thought to be on average about 10^6 times farther away than optical stars, proper motions should be negligible. In addition, the VLBI technique should reach angular measurement accuracies approaching 0.001 arcseconds (5×10^{-9} radians). Hence, VLBI radio reference frames should possess accuracies which exceed those of optical reference frames by one or two orders of magnitude (Refs. 2, 3).

Of what use is such an accurate celestial reference frame? Some examples:

(1) *Calibrating Deep Space Probe Radio Metric Tracking Data* – The DSN is currently developing an operational VLBI system to synchronize clock epochs and rates among the worldwide DSN spacecraft tracking stations and to monitor earth rotational irregularities in order to properly calibrate radio metric navigation data from interplanetary spacecraft (Ref. 4). In addition, the measured variations in earth spin rate and pole position are important clues to understanding the dynamics of the earth's crust and interior (Refs. 5, 6, 7).

(2) *Navigating Interplanetary Spacecraft* – The DSN is currently involved in a demonstration of the value of VLBI measurements of spacecraft position for improving the navigation of the Voyager spacecraft (Ref. 8). Computer simulations have shown that VLBI would provide significant navigational enhancements to future interplanetary missions as well (e.g.: Galileo, VOIR).

(3) *Measuring Planetary and Lunar Orbital Motions* – Improved knowledge of planetary and lunar motion by means of observations of spacecraft in orbit about or on the surface of these bodies will provide higher navigational accuracy for deep space probes as well as useful information for studies of solar system dynamics. At present, JPL researchers are observing the motion of both the moon and Mars by VLBI techniques (Ref. 9).

(4) *Monitoring Earth Crustal Motions* – At JPL, project ARIES is currently demonstrating that VLBI can be used to monitor local crustal motions in order to study their relationship to seismic events (Refs. 10, 11). Eventually, VLBI will be used to measure the relative motion of crustal blocks on a global scale.

(5) *Earth Surveying* – The National Geodetic Survey is considering using VLBI techniques to assist in its effort to accurately determine the relative separations of widely spaced survey markers.

With this justification, we can now consider what the logical steps in the development of a VLBI reference frame would be:

(1) Conduct a sky search for celestial VLBI sources which might be useful.

(2) Choose the "best" subset of these sources for forming the VLBI reference frame.

(3) Determine accurate relative positions of these sources.

Although it is conceptually possible to pursue these tasks in purely sequential order, in practice we have performed these activities to a large extent in parallel. Nonetheless, to date, the most intensive effort has gone into searching for sources, and that is the subject of the remainder of this article.

II. The Search Concept

The search for VLBI sources first became an organized pursuit in the summer of 1974. Up to that point, perhaps 60 celestial VLBI sources had been found by DSN efforts as well as astronomers at other institutions. It became evident that this number of sources would not suffice for future VLBI requirements, and moreover, that this was probably only a small fraction of the total number of VLBI sources in the sky, and hence, probably not an optimum set from which to form a VLBI reference frame. The search began slowly, but in the past two years, increased in intensity. Up to the present time, more than 30 individual observing sessions have been organized.

III. What is a VLBI Source?

The strength of a celestial radio source, or its total flux density, can be expressed as:

$$S_T = \underset{\substack{\text{over the}\\ \text{source}}}{\iint} B(\theta, \phi) d\theta d\phi$$

where

S_T = total flux density in Jansky (1 Jansky = 10^{-26} watts/m^2/Hz)

θ,ϕ = orthogonal angular celestial coordinates measured from a designated source center in radians

$B(\theta,\phi)$ = the angular brightness distribution of the source in Jansky/steradian

The VLBI strength of a celestial radio source, or its correlated flux density, can be expressed as (Ref. 12):

$$S_c = \left| \underset{\substack{\text{over the}\\\text{source}}}{\iint} B(\theta,\phi) e^{-i(2\pi)(u\theta + v\phi)} \, d\theta d\phi \right|$$

where

S_c = correlated flux density in Jansky

u, v = the components of the baseline vector separating the two observing antennas, along θ, ϕ plane of sky coordinates, in RF wavelengths

So, for a particular observation, the correlated flux density is merely the amplitude of one component of a complex two-dimensional spatial Fourier transform of the angular brightness distribution of the source. If the source angular size is significantly smaller than the spatial wavelengths of the transform component, $1/u$ and $1/v$, then it is easy to derive that the correlated flux density is equal to the total flux density. If most of the power emanating from a source comes from angular areas that are large compared to the spatial wavelengths, then virtually none of the total flux density of the source appears as correlated flux density. So, to observe a significant fraction of the total flux density as correlated flux density, much of the total flux density must come from regions smaller than $1/u$ and $1/v$.

Our baselines lengths were about 7×10^7 RF wavelengths, and so the spatial wavelengths, $1/u$ and $1/v$, were generally on the order of a few milliarcseconds. Hence, the radio sources we detect as VLBI sources have a significant amount of their total flux density contained in components that are no more than a few milliarcseconds in angular extent. Only a small percentage of celestial radio sources have such tiny strong components. More typically, radio sources are many seconds of arc to several minutes of arc in angular extent.

What types of celestial sources have such small components? Within our own galaxy there are not many VLBI sources of interest to us. A few molecular clouds emit maser radiation from compact regions (Ref. 13). However, because the molecules radiate at only discrete spectral lines, are extremely time variable, and are relatively nearby, these sources are not the object of our search. Since stars are usually very weak radio sources, few stars have been detected with present VLBI systems (Ref. 14). The only confirmed, reliable, and wideband VLBI source of reasonable strength within our own galaxy is the galactic center source (Ref. 15).

Exterior to our galaxy, VLBI sources within our limits of detectability fall into three categories:

(1) *Quasars* – The most distant class of extragalactic objects. Optically, they are stellar in appearance, with emission and absorption spectral lines shifted far to the red. By current cosmological thought, the large redshifts are indicative of great distance, generally billions of light years. The extraordinary power output per unit volume exhibited by quasars is not explained by current theories. A prominent suggestion is that the large energies are released by matter falling into massive black holes, perhaps as large as 10^8 - 10^{10} solar masses. Ground based VLBI studies indicate that not only do some of these objects possess angular radio structure at the milliarcsecond level, but that this structure can be time-variable over a few months with apparent internal velocities exceeding the speed of light (Ref. 16). Most of the VLBI sources we find are identified as quasars, when optical identifications exist.

(2) *BL Lacertae Type Objects* – These radio sources appear to be similar to quasars, but their atomic emission lines are nonexistent or weak. They are generally somewhat more compact and time-variable than quasars (Ref. 17). Astronomers feel they may be the bright cores of distant elliptical galaxies.

(3) *Galactic Cores* – Many galaxies possess an active central region from which radio emission emanates. VLBI observations have shown that galactic cores can contain angular structure at the milliarcsecond level and, in one case, structural changes which indicate apparent internal velocities exceeding the speed of light (Ref. 16). The VLBI features are often aligned with larger scale features of the source, which suggest that both small and large scale radio structure may have originated from similar explosive events in the core at different epochs. Of perhaps more terrestrial interest is the fact that our own galaxy has an active VLBI core.

The noted similarities of quasars, BL Lacertae objects, and galactic cores may be an indication that all three are merely different classes of a single type of celestial phenomenon, perhaps at different evolutionary stages.

IV. Selection of Candidate Sources

If one were to examine the entire sky for VLBI sources to the level of sensitivity we desire, the task might take several decades. Hence, our search was relegated to observing known celestial radio sources to see which of these might be VLBI sources.

In order to keep from searching all known celestial radio sources for VLBI components, we have used existing information on radio sources as clues to source size. The following criteria proved useful in determining which sources might have structure confined to the milliarcsecond level:

(1) *Spectrum* – Power does not fall off with increasing frequency as rapidly as more typical radio sources in the range 1–10 GHz. An even stronger indicator is if the spectrum is flat, sloped upward, or peaked in this range. Of all the indicators of milliarcsecond structure, spectral properties have proved the most useful.

(2) *Variability* – Identified as radio or optical variable.

(3) *Optical Identification* – Identified as extragalactic.

(4) *Size Limits* – A short baseline interferometer can determine if a source has components smaller than its resolution limit (resolution does not exceed a few arcseconds).

(5) *Interplanetary Scintillation* – Radio sources that show scintillations when viewed through the solar corona possess components with angular sizes $\lesssim 0.1$ arcsecond.

(6) *Detection in High Frequency Surveys* – A larger percentage of sources detected in surveys between 1 and 10 GHz are VLBI sources than is the case at lower frequencies.

We searched the literature for information on celestial radio sources. This was not a simple task, as the information is scattered through hundreds of articles. Nor is the literature static. Many of the high frequency radio surveys have only been performed during the last few years, and some of the sky is still unsurveyed at high frequency. Fortunately, a few high frequency radio surveys (e.g.: Parkes, NRAO-Bonn, Ohio State) provide data on a large fraction of the sky. In general, we chose as candidates only those sources whose total flux densities were greater than 0.7 Jansky at 2.3 GHz.

To date, our literature searches have yielded about 1100 celestial radio sources which might prove to be VLBI sources. Of these, we have performed VLBI observations on almost 900 sources, and have detected 564 as VLBI sources.

V. The Observations

The observations were all performed with pairs of antennas within the DSN which were separated by intercontinental distances. In practice, this meant observing on the Goldstone-Australia or Goldstone-Spain baselines as pairs of antennas on the Spain-Australia baseline cannot simultaneously observe a very large area of sky. Generally, 64 - 26-meter antenna pairs were used, but occasionally 64 - 64-meter combinations were substituted. All the observations were performed at 2290 MHz. The receiver chain generally consisted of an S-band traveling wave maser followed by a special phase stable S-band VLBI receiver which converted the signal to an IF of 50 MHz. The Mark II VLBI recording system, which was developed by the National Radio Astronomy Observatory, then recorded a 1.8 MHz data bandwidth by digitally sampling at a 4-Mbs rate (Ref. 18). Digital sampling and phase stability of the receiver chain were controlled by rubidium or hydrogen maser atomic clocks. System temperatures were measured at both antennas for each source so that the data could be properly calibrated.

VI. Data Processing

Matching tapes from the two antennas were then cross-correlated on a special hardware/software computer at the National Radio Astronomy Observatory in Charlottesville, Virginia. Computer manipulation of the output of this correlator yielded the correlation constant, ρ, for each observation, or the fraction of bits on the two tapes that were correlated. Correlation constants were then converted into correlated flux densities, S_c, by means of the expression:

$$S_c = 2.6\rho \sqrt{T_1 T_2 \left(\frac{dS}{dT}\right)_1 \left(\frac{dS}{dT}\right)_2}$$

where

S_c = correlated flux density in Jansky

T_i = the measured system temperature at antenna i in K

$\left(\frac{dS}{dT}\right)_i$ = the inverse sensitivity of antenna i in Jansky/K (i.e., how strong does a source have to be in total flux density (Jansky) to raise the system temperature 1K)

The uncertainty in the correlated flux density measurements due to random noise effects may be expressed as:

$$\sigma_{S_c} = 6.3 \times 10^3 \sqrt{\frac{T_1 T_2}{e_1 e_2}} \frac{1}{D_1 D_2} \frac{1}{\sqrt{Bt}}$$

where

e_i = the antenna efficiency of antenna i (dimensionless)

D_i = the diameter of antenna i in meters

B = the recorded bandwidth in Hz

t = the coherent integration time in seconds

Most sources were observed for at least three minutes, but for data processing the observations were broken into one minute segments. From this we see that the 5σ detection limit for this search for VLBI sources was about 0.1 Jansky. In addition, one would expect the random uncertainty in detected source strength to be about 0.02 Jansky. However, in practice, systematic errors at the 5 or 10% level dominate the random contribution for most sources.

If a priori source positions are in error, the tapes must be correlated over a range of relative tape delay and delay rate offsets in order to detect a VLBI source. Appropriate searches in these parameters were performed so that the sky was completely searched within 0.5 arcminutes of all nominal source positions. Almost all a priori source position errors should be covered by this degree of position searching. In addition, once detections were achieved, the measured delay and delay rate offsets allowed positional errors to be measured to about one arcsecond, a good level from which to start building a VLBI reference frame.

VII. Results

The reduction of our data is not yet at a complete stage. Accurate source strengths and positions have been calculated for less than half of our detected sources. For the remainder we have strengths accurate to about 20%. Nonetheless, it is useful at this stage to study the general sky distribution of detected sources as a function of source strength. In later articles we will publish catalogs of detected sources.

VIII. The General Sky Distribution

Figures 1a, 1b, and 1c display the general sky distribution of detected VLBI sources as a function of VLBI source strength. The plots show the entire sky, with ±12 hours of right ascension, or celestial longitude, being displayed horizontally, and ±90° of declination, or celestial latitude, being displayed vertically. These maps are equal area representations, so that local spatial densities in one area may be compared to local densities in another.

It should be noted that displaying these source distributions as a function of source strength is fraught with problems, since the strengths of the sources may be uncertain for a number of reasons:

(1) Due to incomplete data reduction, our source strengths are only accurate to about 20% for more than half of the sources.

(2) The total flux density and structure of these sources are often time-variable over months or years.

(3) The correlated flux density may change as a baseline turns with earth rotation. This is due to the fact that changes in the projection of the baseline into the plane of the sky in the source direction can cause different spatial frequencies of the source's brightness distribution to be sampled.

(4) Differences in correlated flux density between different baselines may also be apparent due to the sampling of different spatial frequencies.

Hence, in displaying VLBI sky maps as a function of source strength, our gradations in source strength should be kept quite coarse. Even then, the categories are not crisp. However, although the plots may not show the true strength of a particular source at a certain epoch and on a certain baseline, they do indicate the general densitites of sources as a function of strength.

Figure 1a shows the global distribution of all 564 detected sources. The lower limit of correlated flux strength is about 0.1 Jansky. Several things are evident from this plot:

(1) In general, the distribution is dense and rather uniform.

(2) Pairs of DSN antennas cannot commonly view the sky below $\approx -45°$ declination.

(3) The north polar area is more sparsely populated. This is directly due to a lack of sufficient high frequency surveys in this region to easily identify candidate sources to observe.

(4) The areas near the plane of the galaxy (not shown) are more sparsely populated. This is particularly evident between ±30° declination at right ascensions of about -5 and +7 hours. This is due to the fact that high frequency radio surveys often skip the galactic regions and that interstellar charged particles near the galactic plane can cause intrinsically small sources to be scattered to larger angular sizes.

We should point out that this is not nearly a complete map of the VLBI sky at the level of 0.1 Jansky. Since one of our criteria for choosing candidate sources was to generally only keep sources with total flux densities greater than 0.7 Jansky, we have missed a large number of very compact sources with lower total flux densities.

Figure 1b shows the distribution of 184 sources with correlated flux densities greater than 0.5 Jansky. This is also a rather dense and even distribution, and is a more complete representation of the VLBI sky than was the 0.1 Jansky map.

The DSN Block 1 VLBI System is being developed to calibrate radio metric navigation data from deep space probes (Ref. 4). The sensitivity of this system to VLBI source strength is 0.5 Jansky. In order to conserve antenna time, this system is intended to produce the appropriate calibrations with only 1 or 2 hours of observing on each of two baselines. During that short time span, a single pair of DSN antennas will see only a small segment of sky in common. In order to properly estimate the desired parameters, there must be a good distribution of sources within this small common area of sky. This must be true at any time of day. Hence, this system requires a source catalog of about 100 sources. The number of sources we have found with strengths greater than 0.5 Jansky is nicely matched to the number of required sources.

Figure 1c displays the distribution of 50 sources with correlated flux densities greater than 1.0 Jansky. This is also quite a complete representation of the VLBI sky, but the distribution is no longer very dense. Note that less than 10% of the total number of detected VLBI sources have correlated flux strengths greater than 1.0 Jansky.

The falloff in number of sources with increasing source strength is shown more clearly in the histogram of Fig. 2. The number of sources at source strengths less than 0.5 Jansky is smaller than the true sky distribution, due to our candidate selection criteria and our approximate sensitivity limit of 0.1 Jansky. At the high end of the source strength scale, we see that only 10 sources are stronger than 2.0 Jansky and none are stronger than 4.0 Jansky. The middle range of this histogram, say, 0.5 to 2.0 Jansky, can be approximately described by the expression:

$$N = 50 S_c^{-1.9}$$

where

N = the number of sources stronger than a correlated flux strength of S_c Jansky

If this relationship holds at lower source strengths as well, then we might expect to find perhaps 4000 sources with correlated flux strengths greater than 0.1 Jansky, or seven times our present number of detections.

IX. The Ecliptic Distribution

Figures 3a, 3b, and 3c display the distribution of VLBI sources within 10° of the ecliptic plane. These maps are plotted on rectangular grids rather than equal area representations. The ecliptic plane appears as a sinusoidal-like trace across these plots.

The ecliptic plane is important in solar system astrometric VLBI work, for it is here that planets and spacecraft mostly travel. The motions of these objects may be accurately monitored against the background of VLBI sources by means of the technique of Differential VLBI (ΔVLBI). With ΔVLBI, a spacecraft and an extragalactic VLBI source can be simultaneously observed on the same VLBI baseline. When the VLBI measurements of the two sources are subsequently differenced, most error contributions cancel to a high degree, providing an accurate measure of the angular separation of the two sources. Since the remaining sizes of many of these errors after cancellation are proportional to the angular separation of the two sources, a high density of extragalactic VLBI sources along the ecliptic plane is desirable, so that a source close to the spacecraft is always available. It also follows that operational ΔVLBI systems will probably be required to work at more sensitive levels than is required for the operational system which calibrates radio metric navigation data, so that spacecraft/extragalactic VLBI source separations can be reduced. Ideally, one might desire as many as 100 sources in an ecliptic reference frame, so that a spacecraft would never be more than a few degrees from a useful source.

Figure 3a shows all 166 detected sources within 10° of the ecliptic. The distribution is rather dense and uniform except for the two areas where the galactic plane crosses the ecliptic plane at about 6 and 18 hours of right ascension. It may be possible to increase the density of sources in the galactic regions by observing at X-band rather than S-band, as the scattering effect is thought to be inversely proportional to approximately frequency squared. Also shown are the positions along the ecliptic of the critical events in the Voyager and Galileo missions where ΔVLBI might provide significant navigational advantages.

Figure 3b shows the distribution of 51 sources within 10° of the ecliptic plane which have correlated flux densities greater than 0.5 Jansky. The distribution now becomes relatively sparse in some areas. Figure 3c shows the distribution of the 14 sources with strengths greater than 1.0 Jansky. The distribution is now very sparse as demonstrated by the fact that no sources appear anywhere near the Voyager encounters of Jupiter and the whole Galileo Jupiter orbit phase is almost quasar-free.

X. Summary

We are engaged in a task of searching for a suitable set of celestial radio sources from which a high precision VLBI reference frame may be constructed. The observational portion of this program is nearly completed. We have shown here sky distributions of the 564 detected VLBI sources greater than about 0.1 Jansky and the subset of 166 of these sources which lie within 10° of the ecliptic. These distributions are reasonably dense at the level of 0.5 Jansky and below. The DSN operational VLBI system for calibrating radio metric navigation data will utilize sources stronger than 0.5 Jansky. An operational ΔVLBI system would probably have to employ weaker sources.

Significant data reduction and some observing remains to complete the task of searching for VLBI sources. Published catalogs of VLBI sources, source positions, and correlated flux densities will follow this article. The tasks of choosing the "best" of the available VLBI sources and determining accurate relative positions of the chosen sources are now receiving increased emphasis.

Acknowledgement

We are indebted to the efforts of Radio Science Support Group at the Goldstone DSN complex and to the competent assistance of the personnel at Deep Space Stations 13, 14, 42, 43, 62, and 63. We would also like to thank the Station Directors at these stations for supporting our program, namely E. Jackson (DSS 13), C. Koscielski (DSS 14), T. Reid (DSS 42, 43), J. Urech (DSS 62), and J. Fernandez (DSS 63).

References

1. Kellermann, K. I., "Intercontinental Radio Astronomy," *Scientific American,* 226, 2, pp. 72-83, 1972.
2. Rogers, A. E. E., et al., "Extragalactic Radio Sources: Accurate Positions from Very-Long-Baseline Observations," *Ap. J.,* 186, 1973.
3. Clark, T. A., et al., "Radio Source Positions from Very-Long-Baseline Interferometry Observations," *A.J.,* Vol. 81, No. 8, 1976.
4. Mulhall, B. D. L., "DSN VLBI System Status and Plans," *DSN Progress Report* 42-46, July-August, 1978.
5. Shapiro, I. I., et al., "Transcontinental Baselines and the Rotation of the Earth Measured by Radio Interferometry," *Science,* 186, pp. 920-922, 1974.
6. Fanselow, J. L., et al., "The Goldstone Interferometer for Earth Physics," *DSN Technical Report* 32-1526, Vol. V, pp. 45-57, 1971.
7. Shapiro, I. I., and C. A. Knight, "Geophysical Applications of Long-Baseline Radio Interferometry," *Earthquake Displacement Fields and Rotation of the Earth,* L. Manshina et al., Eds., Reidel Pub. Co., pp. 284-301, 1970.
8. Brunn, D. L., et al., "VLBI Spacecraft Tracking System Demonstration, Part I: Design & Planning," *DSN Progress Report* 42-45, May-June, 1978.

9. Slade, M. A., et al., "ALSEP-Quasar Differential VLBI," *The Moon,* 17, pp. 133-147, 1977.

10. Ong, K. M., et al., "A Demonstration of a Transportable Radio Interferometric Surveying System With 3-cm Accuracy on a 307-m Base Line," *JGR,* Vol. 81, No. 20, pp. 3587-3593, 1976.

11. MacDoran, P. F., "Radio Interferometry for International Study of the Earthquake Mechanism," *Acta Astronautica*, Vol. 1, pp. 1427-1444, 1974.

12. Thomas, J. B., "An Analysis of Long Baseline Radio Interferometry," *JPL Technical Report* 32-1526, Vol. VII.

13. Cook, A. H., *Celestial Masers,* Cambridge University Press, 1977.

14. Clark, T. A., et al., "An Unusually Strong Radio Outburst in ALGOL-VLBI Observations," *Ap. J.,* 206, pp. L107-L111, 1976.

15. Kellermann, K. I., et al., "The Small Radio Source at the Galactic Center," *Ap. J.,* 214, L61-L62, 1977.

16. Wittels, J. J., et al., "Fine Structure of 25 Extragalactic Radio Sources," *Ap. J.,* 196, pp. 13-39, 1975.

17. Disney, M. J., and Veron, P., "BL Lacertae Objects," *Sci. Amer.,* 237, No. 2, 1977.

18. Clark, B. G., "The NRAO Tape-Recorder Interferometer System," *Proceedings of the IEEE,* Vol. 61, No. 9, pp. 1242-1248, 1973.

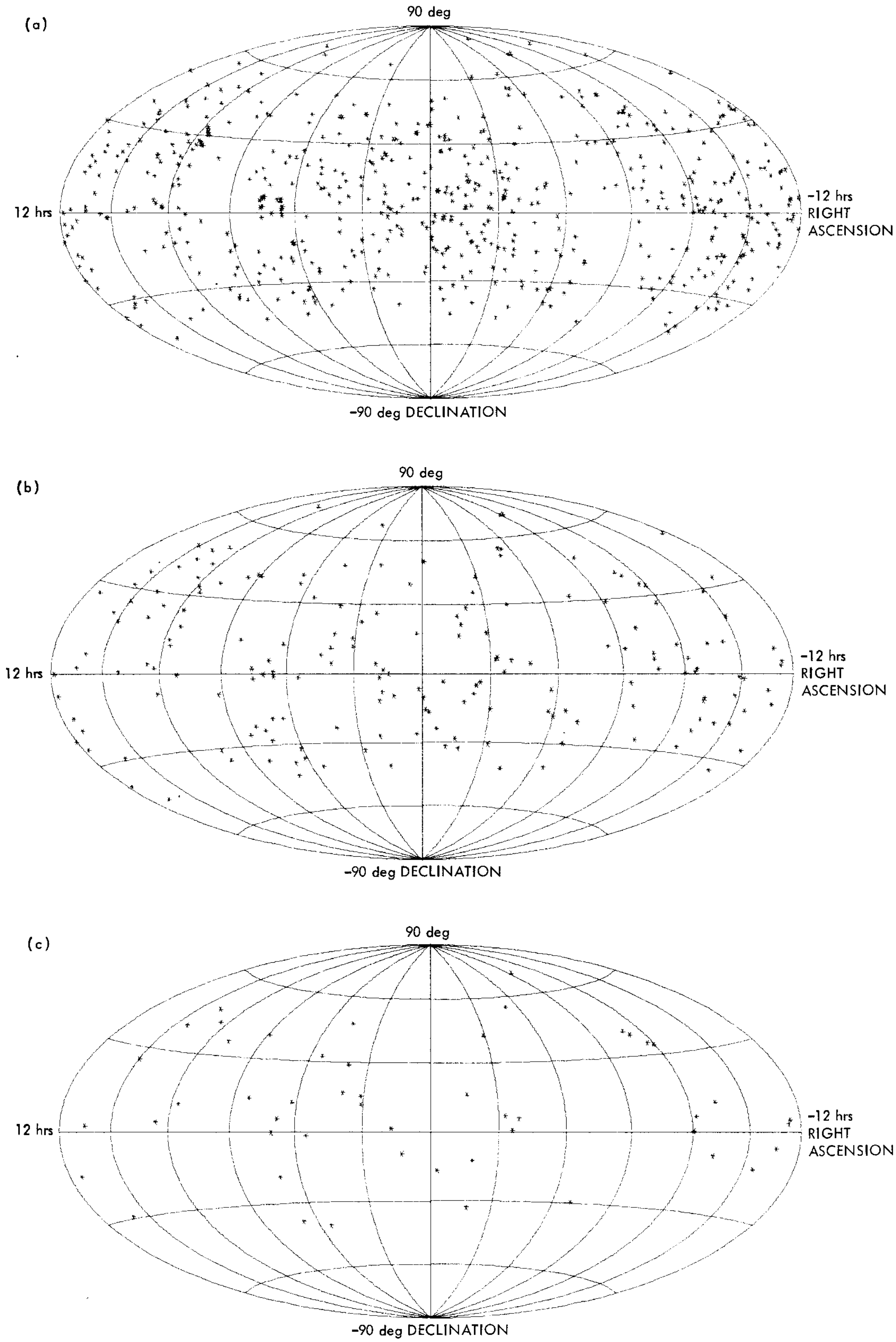

Fig. 1, Sky distribution of VLBI sources: (a) 564 sources ≥0.1 Jansky, (b) 184 sources ≥0.5 Jansky, (c) 50 sources ≥1.0 Jansky

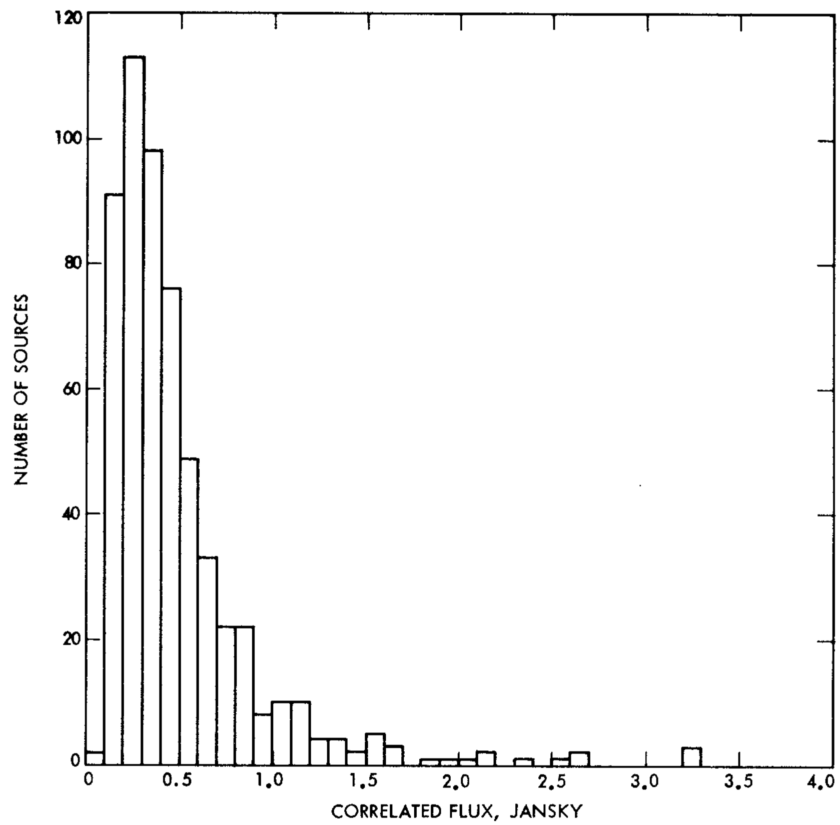

Fig. 2. Histogram of number of VLBI sources versus correlated flux

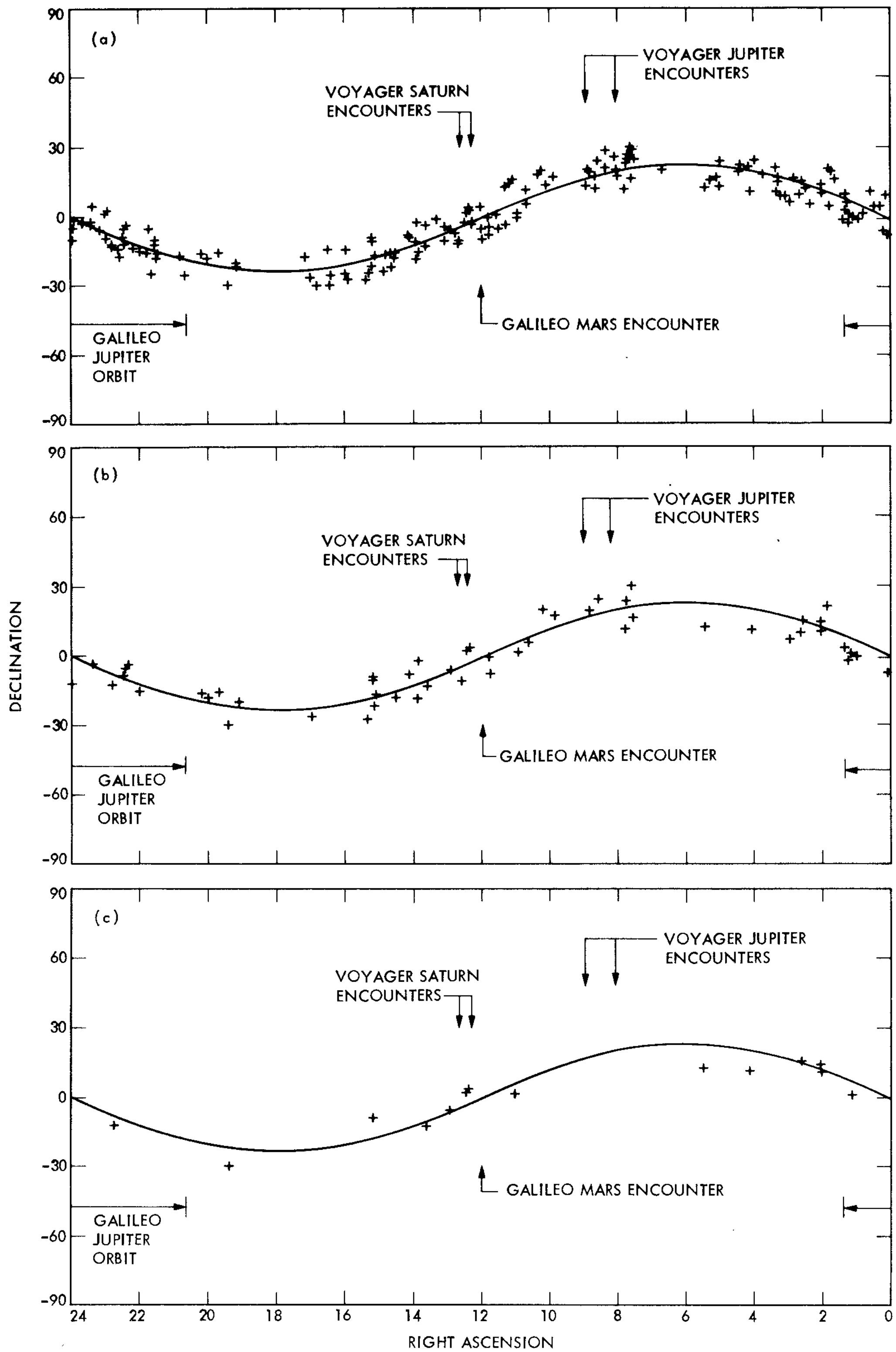

Fig. 3. VLBI sources within ±10° of ecliptic: (a) 166 sources ≥0.1 Jansky, (b) 51 sources ≥0.5 Jansky, (c) 14 sources ≥1.0 Jansky